Journal of Nuclear Medicine, published on October 28, 2013 as doi:10.2967/jnumed.113.121418

^{18}F-FDOPA PET for Differentiating Recurrent or Progressive Brain Metastatic Tumors from Late or Delayed Radiation Injury After Radiation Treatment

Karlo J. Lizarraga[1], Martin Allen-Auerbach[2], Johannes Czernin[2], Antonio A.F. DeSalles[3,4], William H. Yong[5], Michael E. Phelps[2], and Wei Chen[2]

[1]Department of Neurology, Miller School of Medicine, University of Miami, Miami, Florida; [2]Department of Molecular and Medical Pharmacology, David Geffen School of Medicine, UCLA, Los Angeles, California; [3]Department of Neurosurgery, David Geffen School of Medicine, UCLA, Los Angeles, California; [4]Department of Radiation Oncology, David Geffen School of Medicine, UCLA, Los Angeles, California; and [5]Department of Pathology and Laboratory Medicine, David Geffen School of Medicine, UCLA, Los Angeles, California

Brain metastases are frequently treated with radiation. It is critical to distinguish recurrent or progressive brain metastases (RPBM) from late or delayed radiation injury (LDRI). The purpose of this study was to examine the diagnostic accuracy as well as the prognostic power of 6-^{18}F-fluoro-L-dopa (^{18}F-FDOPA) PET for differentiating RPBM from LDRI. **Methods:** Thirty-two patients who had 83 previously irradiated brain metastases and who underwent ^{18}F-FDOPA PET because of an MR imaging–based suggestion of RPBM were studied retrospectively. PET studies were analyzed semiquantitatively (lesion-to-striatum and lesion-to-normal brain tissue ratios based on both maximum and mean standardized uptake values) and visually (4-point scale). The diagnostic accuracy of PET was verified by histopathologic analysis ($n = 9$) or clinical follow-up ($n = 74$) on a lesion-by-lesion basis. Receiver operating characteristic curve analysis was used to identify the best diagnostic indices. The power of ^{18}F-FDOPA PET to predict disease progression was evaluated with the Kaplan–Meier and Cox regression methods. **Results:** The best overall accuracy was achieved by visual scoring, with which a score of 2 or more (lesion uptake greater than or equal to striatum uptake) resulted in a sensitivity of 81.3% and a specificity of 84.3%. Semiquantitative ^{18}F-FDOPA PET uptake indices based on lesion-to-normal brain tissue ratios were significantly higher for RPBM than for LDRI. Among the various predictors tested, ^{18}F-FDOPA PET was the strongest predictor of tumor progression (hazard ratio, 6.26; $P < 0.001$), and the lesion-to-normal brain tissue ratio or visual score was the best discriminator. The mean time to progression was 4.6 times longer for lesions with negative ^{18}F-FDOPA PET results than for lesions with positive ^{18}F-FDOPA PET results (76.5 vs. 16.7 mo; $P < 0.001$). ^{18}F-FDOPA PET findings tended to predict overall survival. **Conclusion:** Metabolic imaging with ^{18}F-FDOPA PET was useful for differentiating RPBM from LDRI. Semiquantitative indices, particularly lesion-to-normal uptake ratios, could be used. A visual score comparing tumor ^{18}F-FDOPA uptake and striatum ^{18}F-FDOPA uptake provided the highest sensitivity and specificity and was predictive of disease progression.

Key Words: ^{18}F-FDOPA PET; brain metastases; radiation treatment; tumor recurrence; radiation injury

J Nucl Med 2014; 55:1–7
DOI: 10.2967/jnumed.113.121418

Brain metastases from systemic cancers arise in 20%–40% of all cancer patients. They account for up to 170,000 new cases per year in the United States (*1*). Primary tumors that are most likely to metastasize to the brain include non–small cell lung cancer (50%), breast cancer (15%–25%), and melanoma (5%–20%) (*2,3*). Prognosis is poor, with reported median survival times of 7–9 mo for metastatic lung cancer (*4*), 2–9 mo for breast cancer (*5*), and 2–5 mo for melanoma (*6*). Patients with solitary lesions have longer survival times than those with multiple lesions (*4–6*).

The management of cerebral metastases usually involves a combination of surgery, radiotherapy, and chemotherapy tailored to individual patients on the basis of the location and number of lesions, performance status, and extent of systemic disease. Radiation therapy can be administered conventionally (whole-brain radiation therapy [WBRT]) or stereotactically (stereotactic radiosurgery [SRS] or stereotactic radiotherapy [SRT]). Most management strategies include surgical excision or SRS plus WBRT (*7*). Thus, most patients with cerebral metastases receive primary, adjunct, or salvage radiation therapy during the course of their disease.

Radiation injury to normal brain tissue is a significant side effect. Classically, radiation injury has been divided into acute and delayed reactions. Late or delayed radiation injury (LDRI) (i.e., "radiation necrosis") has been reported to occur in 3%–24% of patients from 3 mo to 13 y after the completion of radiation therapy (*8*).

After radiation treatment, patients are monitored clinically and radiographically with serial MR imaging. It is challenging to noninvasively distinguish recurrent or progressive brain metastases (RPBM) from LDRI. First, both types of lesions can have similar clinical presentations, such as seizures, focal neurologic deficits, and increased intracranial pressure (*9*). Second, both types of lesions can have similar MR imaging appearances, such as perilesion edema, rimlike enhancement, and central hypointensity on T2-weighted imaging (*9–11*). As opposed to what occurs in RPBM, the enhancement usually becomes more discrete and the lesion

Received Feb. 7, 2013; revision accepted Jul. 25, 2013.
For correspondence or reprints contact: Karlo J. Lizarraga, Department of Neurology, Miller School of Medicine, University of Miami, Clinical Research Building, 1120 N.W. 14th St., 13th Floor, Miami, FL 33136.
E-mail: klizarraga@med.miami.edu
Published online ■■■■■■■■■■■■.

volume tends to decrease with time in LDRI (*9–12*). Treatment options, including invasive modalities, differ for RPBM and LDRI. Therefore, accurate and timely differentiation of these 2 types of lesions can significantly affect patient care and outcome.

PET provides metabolic information that can be used to differentiate RPBM from LDRI (*13*). ^{18}F-FDG PET has been used with variable success because of the high normal glucose metabolic activity of the brain (*14,15*). More promising results—mostly in the setting of primary brain tumors—have been reported with the amino acid PET tracers ^{11}C-methionine (*16*) and *O*-(2-^{18}F-fluoroethyl)-L-tyrosine (^{18}F-FET) (*17*). Preliminary results of PET imaging with 6-^{18}F-fluoro-L-dopa (^{18}F-FDOPA) have also been promising (*18*).

The aims of this study were to assess the diagnostic accuracy of ^{18}F-FDOPA PET imaging for the differentiation of RPBM from LDRI in patients whose brain metastases were treated with radiation and to evaluate the prognostic power of ^{18}F-FDOPA PET imaging in predicting progression-free survival and overall survival.

MATERIALS AND METHODS

Patients and Lesions

From November 2004 to March 2012, 32 patients (26 women and 6 men) with 83 irradiated brain metastases were studied with ^{18}F-FDOPA PET. The institutional review board approved this retrospective study, and the requirement to obtain informed consent was waived. [**Table 1**] The characteristics of the patients are summarized in Table 1. The median age was 58 y (range, 21–77 y). Primary tumors were lung (11 patients; 34 lesions), breast (11 patients; 29 lesions), thyroid (3 patients; 6 lesions), melanoma (3 patients; 4 lesions), testis (2 patients; 3 lesions), ovary (1 patient; 6 lesions), and colon (1 patient; 1 lesion) cancers.

All patients had undergone radiation therapy (SRS, 50 lesions; SRT, 3 lesions; WBRT, 12 lesions; WBRT plus SRS, 18 lesions) before the PET scan. Median treatment doses were 18 Gy for SRS (range, 9–25 Gy), 30 Gy for SRT (range, 24–30 Gy, in 6–10 fractions), and 37.5 Gy for WBRT (range, 30–45 Gy, in 15–18 fractions). SRT was administered as a postoperative boost to the tumor bed in all cases. The median time interval from the completion of radiation treatment to PET was 13.7 mo (range, 3.7–112.5 mo).

Patients were referred for ^{18}F-FDOPA PET imaging to distinguish LDRI from RPBM suggested by MR imaging or clinical symptoms. Nine patients (27 lesions) were treated with corticosteroids on the basis of a change in symptoms and were still receiving corticosteroids at the time of PET.

^{18}F-FDOPA PET

PET was performed on a dedicated system (ECAT HR or HR+; Siemens) for 13 patients; the remaining 19 patients were imaged with a dual-detector PET/CT system (Biograph Duo; Siemens). The dedicated PET system was equipped with bismuth germinate crystal detectors, and the PET/CT system was equipped with lutetium oxyorthosilicate crystal detectors and a dual-detector helical CT scanner. Phantom studies ascertained that activities measured with both scanners were comparable (mean difference of 2.5% in each case). Patients were asked to fast for at least 4 h before image acquisition. ^{18}F-FDOPA was synthesized according to previously reported procedures (*19,20*) and was injected intravenously at a dose of 1.1–6.6 MBq/kg.

For dedicated PET, data were acquired in a 3-dimensional mode. Attenuation correction was calculated as reported previously (*21*). For PET/CT, a CT scan (120 kV, 80 mAs, 1-s tube rotation, 3-mm slice collimation) was acquired first. The CT data were used for attenuation correction as reported previously (*22*). For both PET and PET/CT scans, the emission scan was started 10 min after tracer injection. Images were acquired for 30 min in the 3-dimensional mode. Image data acquired between 10 and 30 min were summed to obtain a 20-min static image. PET images were reconstructed by use of iterative techniques with ordered-subset expectation maximization consisting of 6 iterations with 8 subsets (*23*). A gaussian filter with a full width at half maximum of 4 mm was applied. Radiotracer uptake was normalized to the injected dose per kilogram of patient's body weight to obtain the standardized uptake value (SUV).

Image Analysis

Two experienced nuclear medicine physicians unaware of the clinical information interpreted the PET scans independently by using MR images acquired within 1 wk before the PET scans as a reference. PET images were coregistered with MR images. Images were first inspected visually. The axial PET image slice displaying the maximum lesion ^{18}F-FDOPA uptake was selected and compared with the axial PET image slice displaying the maximum striatum ^{18}F-FDOPA uptake. Both semiquantitative and qualitative approaches were applied for image analysis.

TABLE 1
Characteristics of Patients and Lesions Studied with ^{18}F-FDOPA PET

Characteristic	Median	Range	*n*
Sex			
Women			26
Men			6
Total			32
Age (y) at time of ^{18}F-FDOPA PET imaging	58	21–77	
Patients with primary tumors*			
Lung			11 (34)
NSCLC			9
Adenocarcinoma			2
Breast			11 (29)
Ductal			9
Lobular			1
Inflammatory			1
Thyroid†			3 (6)
Melanoma			3 (4)
Testis			2 (3)
Ovary			1 (6)
Colorectal			1 (1)
Total			32 (83)
Lesions per patient	2	1–6	
Type of radiation therapy received before PET‡			
SRS			50
SRT§			3
WBRT			12
WBRT and SRS			18
Radiation dose (Gy) received before PET			
SRS	18	9–25	
SRT‖	30	24–30	
WBRT¶	37.5	30–45	
Time (mo) from last radiation treatment to PET	13.7	3.7–112.5	

*Values in parentheses are numbers of lesions.
†Papillary.
‡Reported as numbers of lesions.
§Postoperative boost to tumor bed in all cases.
‖In 6–10 fractions.
¶In 15–18 fractions.
NSCLC = non–small cell lung cancer.

jnm121418-pe ■ 10/24/13

TABLE 2
Final Diagnosis of Lesions Studied with ^{18}F-FDOPA PET

Criterion	RPBM	LDRI	Total
Pathologic analysis	7	2	9
Clinical or radiologic course	25	49	74
Total	32	51	83

Values are reported as numbers of lesions.

For semiquantitative analysis, a 10-mm circular region was placed over the area with the peak activity. This region of interest was used to derive the maximum SUV (SUV_{max}) and the mean SUV (SUV_{mean}). Normal reference regions were defined in 2 ways. For the determination of tracer uptake in normal striatum, a region of interest was obtained by drawing an 80% peak-voxel-intensity isocontour over the contralateral striatum. The normal reference brain region was defined by drawing a region of interest involving the entire contralateral hemisphere at the level of the centrum semiovale to derive tumor-to-normal hemispheric brain tissue ratios as described previously (*18*). These normal reference regions were used to derive maximum lesion-to-striatum (L/S_{max}), mean lesion-to-striatum (L/S_{mean}), maximum lesion-to-normal (L/N_{max}), and mean lesion-to-normal (L/N_{mean}) uptake ratios.

For qualitative analysis, a 4-point visual scale was proposed and used to qualify lesions as follows: 0, lesion not visible on PET; 1, lesion visible but uptake less than striatum uptake; 2, lesion uptake and striatum uptake isointense; and 3, lesion uptake greater than striatum uptake.

Final Diagnosis and Follow-up of Patients

Patients were monitored clinically at least every 3 mo unless otherwise indicated by symptoms. PET findings were validated with a pathologic diagnosis of samples from surgical resection (9 lesions) or the radiologic course (74 lesions) within 6 mo of the PET scans. For patients who underwent surgical resection, the available tissue from excised tumors was fixed with formalin overnight (12–18 h) and embedded in paraffin. The paraffin blocks were cut into 5-μm-thick sections. All sections were stained with hematoxylin and eosin. A board-certified neuropathologist reviewed the samples to determine the presence of tumor, necrosis, and sequelae of radiation effects, including hyaline and fibrinoid changes in blood vessels, atypia of brain cells, and necrotic brain tissue associated with these findings.

For patients who did not undergo surgery, the radiographic diagnosis was determined as follows. Lesions that showed shrinkage or remained stable on contrast-enhanced, T1-weighted MR imaging after at least 6 mo of follow-up were considered to be LDRI (*9–12*), whereas lesions that showed increases in volume of 25% or more were considered to represent RPBM (*24,25*). Maximum enhanced lesion diameters in 3 orthogonal planes (sagittal [d1], axial [d2], and coronal [d3]) were used to calculate lesion ellipsoid volumes with the formula $(4/3) \times \pi[(d1 \times d2 \times d3)/2]$ (*24*).

Follow-up of patients was continued after diagnosis for outcome assessment. Progression-free survival and overall survival were calculated from the date of the baseline PET scan to the date of progression or death or to the date of the last follow-up, which was June 15, 2012.

Statistical Analysis

Statistical analysis was performed with PASW software (version 18.0; IBM). Significance was defined as a probability value of less than 0.05. The values of the ^{18}F-FDOPA PET semiquantitative indices for RPBM and LDRI were compared with the Student *t* test. Receiver operating characteristic curve analysis was used to identify the optimal cutoff values of the various ^{18}F-FDOPA PET indices for the differential diagnosis of RPBM versus LDRI. Threshold values were selected when the product of their respective sensitivities and specificities reached its maximum while both sensitivity and specificity were optimized.

The prognostic power of ^{18}F-FDOPA PET in predicting progression-free survival and overall survival was analyzed by use of the Kaplan–Meier and Cox regression methods. Cox regression analysis was also used to compare the predictive power of ^{18}F-FDOPA PET with that of other outcome predictors, such as age, primary tumor type, prior radiation treatment modality (stereotactic, conventional, or stereotactic and conventional), time from radiation treatment completion to PET, and steroid use.

RESULTS

Final Diagnosis

The final diagnosis of RPBM versus LDRI is summarized in Table 2. Nine lesions were surgically resected, with a median time from PET to resection of 35.5 d (range, 16–65 d). The radiologic course established the final diagnosis for the remaining 74 lesions. Thirty-two lesions were considered to be RPBM (32/83 [38.6%]), and 51 lesions were considered to be LDRI (51/83 [61.4%]). [**Table 2**]

^{18}F-FDOPA Uptake Indices

^{18}F-FDOPA uptake was quantified as SUV_{mean}, SUV_{max}, L/S_{mean}, L/S_{max}, L/N_{mean}, and L/N_{max}. Furthermore, lesions were scored visually as described earlier. Four examples are shown in Figure 1. [**Fig. 1**]

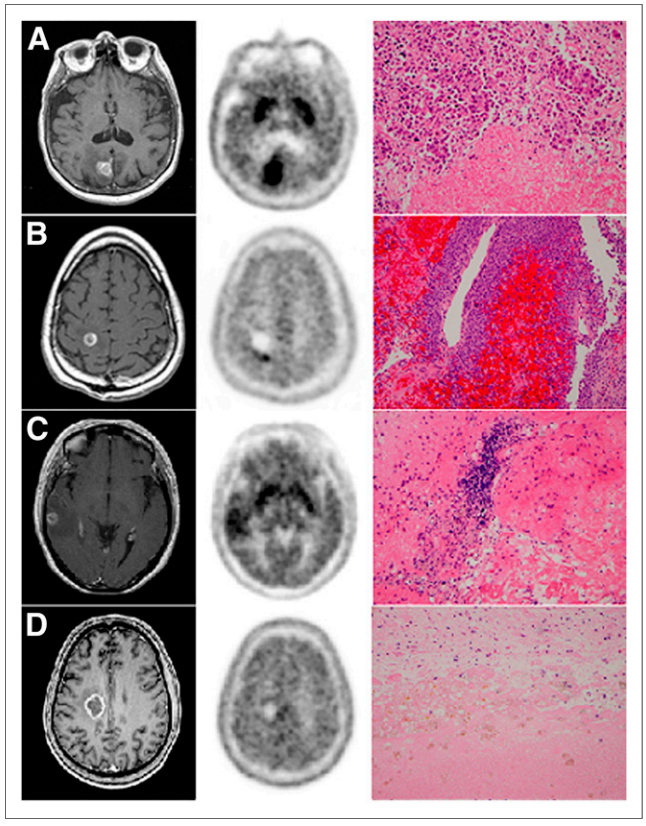

FIGURE 1. Illustrative examples. (A) L/N_{max}, 3.53; L/N_{mean}, 3.20; L/S_{max}, 1.24; L/S_{mean}, 1.67; visual scale score, 3; biopsy, RPBM (breast). (B) L/N_{max}, 2.31; L/N_{mean}, 1.76; L/S_{max}, 1.06; L/S_{mean}, 0.99; visual scale score, 2; biopsy, RPMB plus hemorrhage (melanoma). (C) L/N_{max}, 2.04; L/N_{mean}, 1.73; L/S_{max}, 0.88; L/S_{mean}, 0.94; visual scale score, 1; biopsy, LDRI plus inflammatory cells (lung). (D) L/N_{max}, 1.75; L/N_{mean}, 1.31; L/S_{max}, 0.62; L/S_{mean}, 0.63; visual scale score, 1; biopsy, LDRI plus hemosiderin macrophages (testis).

[Table 3] Semiquantitative PET scan data are shown in Table 3. All PET uptake indices were significantly higher for RPBM than for LDRI, particularly when lesions had been previously irradiated stereotactically.

[Table 4] Table 4 summarizes the receiver operating characteristic curve analysis of the ^{18}F-FDOPA PET indices. The qualitative visual score provided the best sensitivity and specificity. When this visual scale was used, a score threshold of greater than or equal to 2 (i.e., uptake equal to or higher than that of the striatum) resulted in a sensitivity of 81.3%, a specificity of 84.3%, and an accuracy of 83.1% for differentiating RPBM from LDRI. Among the semiquantitative indices, the L/N_{max} and L/N_{mean} uptake ratios had the highest accuracy (75.9%) for differentiating RPBM from LDRI. A sensitivity of 81.3% and a specificity of 72.5% were obtained with both L/N_{max} values of greater than or equal to 2.02 and L/N_{mean} values of greater than or equal to 1.70.

Predictive Value of ^{18}F-FDOPA PET

The probability of disease progression determined with the visual [Fig. 2] scale is shown in Figure 2. A positive PET reading (defined by a visual scale score of greater than or equal to 2) had significant predictive power for time to progression of the evaluated lesion ($P < 0.001$, as determined with the log rank test). The predictive power for progression in a patient-based analysis was also significant ($P < 0.05$, as determined with the log rank test). There was a significant difference in mean time to progression between lesions with positive PET results (visual scale score of 2 or 3; 16.7 mo) and lesions with negative PET results (visual scale score of 0 or 1; 76.5 mo) ($P < 0.001$). There was a trend toward better survival for patients who had lesions with negative PET results ($P = 0.06$, as determined with the log rank test).

[Table 5] The univariate Cox regression analysis (Table 5) showed that prior conventional radiation treatment ($P < 0.001$), time from radiation treatment completion to ^{18}F-FDOPA PET imaging of less than 6 mo ($P = 0.003$), and positive ^{18}F-FDOPA PET results ($P < 0.001$) were predictive of progression, with hazard ratios of 4.54, 3.64, and 6.95, respectively. The multivariate analysis showed that only prior conventional treatment ($P = 0.005$) and positive PET results ($P < 0.001$) were predictive of progression, with hazard ratios of 3.50 and 6.26, respectively.

Other clinical factors, such as a patient's age ($P = 0.306$), primary tumor type ($P = 0.217$), prior stereotactic radiation treatment ($P = 0.083$), prior stereotactic and conventional radiation treatments ($P = 0.521$), and steroid use during PET imaging ($P = 0.449$), were not predictive (Table 5).

DISCUSSION

To our knowledge, this is the first study to investigate the diagnostic value of ^{18}F-FDOPA PET for the differentiation of RPBM from LDRI in metastatic brain tumors. First, the results of the present study demonstrated that ^{18}F-FDOPA PET could distinguish between RPBM and LDRI with a high diagnostic accuracy—83.1% (sensitivity, 81.3%; specificity, 84.3%)—in a population of patients in whom RPBM was suggested by MR imaging. Second, evaluation with ^{18}F-FDOPA PET was highly prognostic of progression-free survival. Lesions with negative ^{18}F-FDOPA PET results had a mean time to progression that was 4.6 times longer than that of lesions with positive ^{18}F-FDOPA PET results (76.5 mo vs. 16.7 mo; $P < 0.001$). Third, both semiquantitative indices (L/N_{max} and L/N_{mean}) and the qualitative assessment (visual scale score) comparing the intensity of lesion uptake with the intensity of striatum uptake performed comparably well in providing diagnosis and prognosis. Fourth, a trend toward predicting overall survival was seen.

^{18}F-FDG was the first PET tracer used to distinguish RPBM from LDRI (*26*). A sensitivity of 65% and a specificity of 80% were reported (*14*). ^{18}F-FDG uptake by normal cerebral cortex is high and variable. In addition, ^{18}F-FDG uptake can be modified by

TABLE 3
Semiquantitative Analysis of ^{18}F-FDOPA PET Imaging Data

Index	RPBM Mean	RPBM SD	LDRI Mean	LDRI SD	P*
Lesion SUV_{max}	3.57	1.27	2.17	0.83	<0.05
Stereotactic	3.52	1.20	2.16	0.88	<0.05
Conventional	3.57	0.89	1.55	0.95	<0.05
Conventional and stereotactic	3.69	1.91	2.36	0.57	0.12
Lesion SUV_{mean}	2.91	0.99	1.82	0.77	<0.05
Stereotactic	3.01	1.05	1.83	0.81	<0.05
Conventional	2.80	0.57	1.32	0.86	0.08
Conventional and stereotactic	2.82	1.36	1.95	0.58	0.15
Striatum SUV_{max}	3.25	0.89	3.16	1.11	0.71
Stereotactic	3.42	0.95	3.27	1.22	0.64
Conventional	3.48	0.60	2.35	0.99	0.18
Conventional and stereotactic	2.57	0.83	3.01	0.60	0.25
Striatum SUV_{mean}	2.55	0.69	2.47	0.87	0.65
Stereotactic	2.70	0.78	2.54	0.96	0.57
Conventional	2.65	0.41	1.95	0.63	0.18
Conventional and stereotactic	2.09	0.62	2.39	0.48	0.26
Normal brain SUV_{max}	1.34	0.33	1.29	0.49	0.49
Stereotactic	1.37	0.30	1.35	0.49	0.88
Conventional	1.15	0.26	0.79	0.59	0.17
Conventional and stereotactic	1.13	0.40	1.20	0.39	0.71
Normal brain SUV_{mean}	0.95	0.38	0.93	0.23	0.76
Stereotactic	1.01	0.20	0.99	0.39	0.81
Conventional	0.86	0.17	0.50	0.28	0.15
Conventional and stereotactic	0.82	0.32	0.92	0.30	0.55
L/S_{max}	1.14	0.39	0.72	0.29	<0.05
Stereotactic	1.07	0.38	0.69	0.26	<0.05
Conventional	1.03	0.20	0.71	0.54	0.41
Conventional and stereotactic	1.43	0.50	0.82	0.29	<0.05
L/S_{mean}	1.18	0.39	0.76	0.30	<0.05
Stereotactic	1.16	0.42	0.75	0.30	<0.05
Conventional	1.05	0.14	0.71	0.56	0.39
Conventional and stereotactic	1.37	0.53	0.83	0.25	<0.05
L/N_{max}	2.72	0.95	1.81	0.94	<0.05
Stereotactic	2.61	0.88	1.63	0.51	<0.05
Conventional	1.88	0.26	2.17	2.16	0.84
Conventional and stereotactic	3.36	1.32	2.24	1.40	0.11
L/N_{mean}	2.24	0.84	1.52	0.81	<0.05
Stereotactic	2.23	0.75	1.37	0.47	<0.05
Conventional	2.40	0.49	2.50	2.31	0.95
Conventional and stereotactic	2.70	1.33	1.83	1.12	0.17

*As determined by *t* test.

jnm121418-pe ■ 10/24/13

TABLE 4
Receiver Operating Characteristic Curve Analysis of ^{18}F-FDOPA PET Diagnostic Criteria for Differentiating RPBM from LDRI

Diagnostic criterion	Area under curve	Confidence interval	Threshold for RPBM	Sensitivity*	Specificity*	Positive predictive value*	Negative predictive value*	Accuracy*
SUV_{max}	0.822	0.732–0.913	≥2.74	68.8 (22/32)	68.6 (35/51)	57.9 (22/38)	77.8 (35/45)	68.7
SUV_{mean}	0.822	0.733–0.911	≥2.3	68.8 (22/32)	70.6 (36/51)	59.5 (22/37)	78.3 (36/46)	69.9
L/S_{max}	0.837	0.753–0.921	≥0.86	75.0 (24/32)	72.5 (37/51)	63.2 (24/38)	82.2 (37/45)	73.5
L/S_{mean}	0.823	0.736–0.910	≥0.95	68.8 (22/32)	76.5 (39/51)	64.7 (22/34)	79.6 (39/49)	73.5
L/N_{max}	0.837	0.753–0.922	≥2.02	81.3 (26/32)	72.5 (37/51)	65.0 (26/40)	86.0 (37/43)	75.9
L/N_{mean}	0.829	0.743–0.916	≥1.70	81.3 (26/32)	72.5 (37/51)	65.0 (26/40)	86.0 (37/43)	75.9
Visual scale	0.892	0.824–0.960	≥2	81.3 (26/32)	84.3 (43/51)	76.5 (26/34)	87.8 (43/49)	83.1

*Reported as percentage.

nonneoplastic and radiation-related effects (inflammation, radiation injury, repair mechanisms, chemotherapy, and steroid treatment) (*14,15,27*). It was hypothesized that delineation of gliomas from gray matter with ^{18}F-FDG PET could be improved by extending the interval between ^{18}F-FDG administration and PET data acquisition (*28*). Indeed, in 12 of 19 patients studied, visual analysis showed that delayed images—obtained at 180–240 min after injection—better distinguished the high uptake in tumors relative to the uptake in gray matter. SUV comparisons also revealed higher uptake in tumors than in gray matter, brain, or white matter at delayed times (*28*). Furthermore, delayed imaging with ^{18}F-FDG PET was investigated in 22 patients with previously irradiated gliomas being evaluated for recurrence versus necrosis (*29*). Regardless of histologic type, the differentiation of necrosis from metastatic brain lesions was improved by use of the change in the ratio of lesion SUV_{max} to gray matter SUV_{max} as a function of time.

^{18}F-FDOPA is an amino acid analog PET tracer that is taken up by brain tumors because of increased amino acid transport in tumor tissue (*17,30–33*). The increased uptake in tumor tissue is most likely purely due to this increased transport, without involving a dopaminergic metabolism, because uptake time–activity curves showed a pattern different from that of striatum (*18,31*). In fact, in one of our early studies (*18*), the diagnostic accuracy of ^{18}F-FDOPA PET was examined in 81 patients with gliomas by comparison of indices based on SUV_{max}, SUV_{mean}, tumor-to-striatum ratio, tumor-to-normal hemisphere ratio, and tumor-to-normal white matter ratio. The conclusion was that all of these indices had comparable diagnostic accuracies. The idea of using a visual scale based on the lesion-to-striatum ratio came from clinicians. Although it is true that, because of its intrinsic dopaminergic metabolism, background striatum ^{18}F-FDOPA uptake could be influenced by several physiologic, pharmacologic, and pathophysiologic processes (*34*), it could prove practically useful by providing an internal reference standard for clinically applicable visual scale scoring. This simple and clinically practical approach would be especially useful when ^{18}F-FDOPA uptake quantitative measurements are not available, such as in a clinic setting. In fact, the proposed qualitative visual scale provided the best results overall in the present study.

Studies in which amino acid PET tracers have been used to distinguish recurrent tumor from radiation-induced changes are limited. ^{11}C-methionine is the amino acid analog PET tracer that has been studied the most. In 1 study, a sensitivity of 77.8% and a specificity of 100% were obtained, with a mean uptake ratio threshold of 1.41, for distinguishing RPBM from LDRI (*16*). In a second, larger study, a sensitivity of 79% and a specificity of 75%, with a similar cutoff value, were reported (*35*). ^{18}F-FET PET was recently reported to have a similar sensitivity (74%) and improved specificity (90%), with a mean uptake ratio threshold of 1.95 (*36*). Our findings of an ^{18}F-FDOPA L/N_{max} of greater than or equal to 2.02 and an L/N_{mean} of greater than or equal to 1.70, providing a sensitivity of 81.3% and a specificity of 72.5%, are consistent with the findings of these earlier studies. Notably, the addition of tracer kinetic analysis and time–activity curve patterns of ^{18}F-FET PET significantly improved both sensitivity (84%) and specificity (100%) (*36*).

A multivariate analysis showed 2 significant predictors of progression. In addition to having positive ^{18}F-FDOPA PET results, lesions previously treated with conventional radiation (i.e., WBRT) alone were 3.5 times more likely to progress ($P < 0.005$) (Table 5). Significantly better local control with WBRT plus SRS than with WBRT alone has been discussed elsewhere (*37*). In addition,

jnm121418-pe ■ 10/24/13

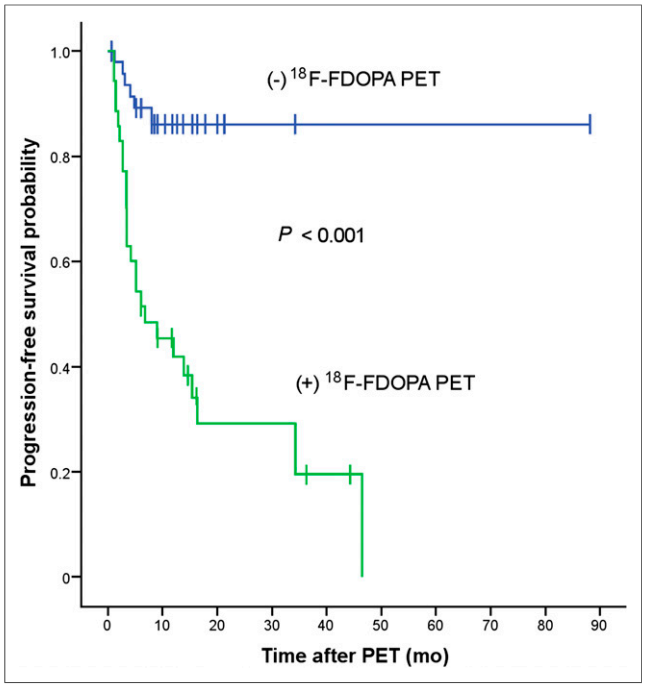

FIGURE 2. Predictive power of proposed ^{18}F-FDOPA PET visual scale for lesion progression, as calculated by Kaplan–Meier method.

patients who were treated with WBRT might have had more severe disease than those treated with SRS alone. Only a trend for predicting overall survival was seen ($P = 0.06$). This result was not surprising because the mortality of patients with metastatic brain tumors can result from systemic disease as well. Finally, a time from radiation completion to PET imaging of less than 6 mo was predictive of progression in the univariate analysis but not in the multivariate analysis. This loss of significance might have been due to the presence of other variables, such as a higher likelihood of RPBM versus LDRI in this time period (*7,37*).

Different radiation therapy modalities (e.g., WBRT, SRS, and SRT) might affect ^{18}F-FDOPA uptake differently in normal brain tissue. Interestingly, in the LDRI group, striatum ^{18}F-FDOPA uptake was lower in patients treated with WBRT than in those treated with stereotactic radiation (Table 3). This result could have been due to reduced amino acid transport in normal tissue affected by radiation in WBRT, because stereotactic radiation targets tumors more focally. Moreover, the effects of radiation might include specific dopaminergic alterations. Remarkably, in both the LDRI group and the RPBM group, normal brain uptake indices were also lower in patients treated with WBRT than in those treated with stereotactic radiation alone (Table 3). Further studies are needed to establish whether and how the radiation modality influences ^{18}F-FDOPA uptake in normal brain tissue, RPBM, and LDRI.

False-negative PET scan results could be caused by smaller lesions, variability in the upregulation of amino acid transport among different tumors, or different cell proliferation rates. False-positive ^{18}F-FDOPA findings might have arisen from previous treatment effects, such as breakdown of the blood–brain barrier, which could increase tumor ^{18}F-FDOPA uptake (*38*). Moreover, inflammation might affect ^{18}F-FDOPA uptake in normal tissue, an issue that has not been investigated to date. Steroid therapy, age, and tumor type were not predictive of progression in the present study. Determining the predictive significance of these factors for progression requires further investigation.

The present study has several limitations. First, the study population was small. Second, the retrospective nature of the study could have introduced selection bias. Third, the time between the completion of radiation treatment and PET had a long range, from 4 mo to 9 y. Although LDRI has been reported up to 13 y after radiation (*8*), the probabilities of RPBM and LDRI may vary considerably in this time period. Fourth, MR imaging and PET imaging techniques have evolved in this time period. Fifth, because multiple lesions occur frequently in cerebral metastases and biopsy is usually not performed for all lesions, pathologic verification was available only in a small subset of patients and radiologic criteria were used for the final diagnosis in a large percentage of patients. However, with hybrid technologies such as PET/CT or software fusion of PET and MR images, localization and follow-up of lesions are feasible. Finally, the image analysis method and the radiologic criteria used to determine the final diagnosis have not been standardized (*24,25*).

TABLE 5
Cox Regression Analysis of Probability of Lesion Progression After ^{18}F-FDOPA PET Imaging

	Univariate analysis			Multivariate analysis		
Predictive factor	Hazard ratio	95% confidence interval	*P*	Hazard ratio	95% confidence interval	*P*
Age	1.02	0.99–1.05	0.31			
Primary tumor vs. lung			0.976			
Breast	1.04	0.49–2.34				
Other	1.11	0.45–2.71				
Prior stereotactic radiation treatment	0.53	0.26–1.09	0.08			
Prior conventional radiation treatment	4.55	1.97–10.50	<0.01	3.46	1.27–9.44	0.015
Prior stereotactic and conventional radiation treatments	0.75	0.30–1.83	0.52			
<6 mo from radiation treatment completion to PET	3.64	1.54–8.62	<0.01	1.02	0.36–2.90	0.97
≥12 mo from radiation treatment completion to PET	0.68	0.34–1.37	0.28			
Steroid treatment during PET	1.32	0.64–2.73	0.50			
Positive PET result (visual scale score of ≥2)	6.95	2.86–16.93	<0.01	6.24	2.51–15.47	<0.01

jnm121418-pe ■ 10/24/13

PET measurements may be affected by clinical as well as technical variables. In addition, the possible coexistence of RPBM and LDRI in the same lesion can render quantitative measurements even more complicated. Hence, the implementation of standard cutoff values across multiple centers can be challenging. The use of visual scales and lesion-to-normal tissue ratios, such as those proposed in the present study, represents a practical approach that could be easily implemented in routine clinical practice.

CONCLUSION

Metabolic imaging with ^{18}F-FDOPA PET provided high diagnostic accuracy for differentiating RPBM from LDRI. Semiquantitative parameters, particularly an L/N_{max} of greater than or equal to 2.02 and an L/N_{mean} of greater than or equal to 1.70, were useful. However, a qualitative visual scale score of greater than or equal to 2 (i.e., lesion uptake equal to or higher than contralateral striatum uptake) was best at predicting the course of the disease. These findings need to be validated in larger prospective studies.

DISCLOSURE

The costs of publication of this article were defrayed in part by the payment of page charges. Therefore, and solely to indicate this fact, this article is hereby marked "advertisement" in accordance with 18 USC section 1734. This study was supported in part by institutional funding at the Department of Molecular and Medical Pharmacology, David Geffen School of Medicine, UCLA. No other potential conflict of interest relevant to this article was reported.

ACKNOWLEDGMENTS

We thank Dr. David Elashoff and Tristan Grogan, Department of General Internal Medicine, David Geffen School of Medicine, UCLA, for statistical review of the article.

REFERENCES

1. Gavrilovic IT, Posner JB. Brain metastases: epidemiology and pathophysiology. *J Neurooncol.* 2005;75:5–14.
2. Barnholtz-Sloan JS, Sloan AE, Davis FG, Vigneau FD, Lai P, Sawaya RE. Incidence proportions of brain metastases in patients diagnosed (1973 to 2001) in the Metropolitan Detroit Cancer Surveillance System. *J Clin Oncol.* 2004;22:2865–2872.
3. Cavaliere R, Schiff D. Cerebral metastases: a therapeutic update. *Nat Clin Pract Neurol.* 2006;2:426–436.
4. Oh Y, Taylor S, Bekele BN, et al. Number of metastatic sites is a strong predictor of survival in patients with nonsmall cell lung cancer with or without brain metastases. *Cancer.* 2009;115:2930–2938.
5. Brogi E, Murphy CG, Johnson ML, et al. Breast carcinoma with brain metastases: clinical analysis and immunoprofile on tissue microarrays. *Ann Oncol.* 2011; 22:2597–2603.
6. Meier S, Baumert BG, Maier T, et al. Survival and prognostic factors in patients with brain metastases from malignant melanoma. *Onkologie.* 2004;27:145–149.
7. Ellis TL, Neal MT, Chan MD. The role of surgery, radiosurgery and whole brain radiation therapy in the management of patients with metastatic brain tumors. *Int J Surg Oncol*. 2012;2012:952345.
8. Ruben JD, Dally M, Bailey M, Smith R, McLean CA, Fedele P. Cerebral radiation necrosis: incidence, outcomes, and risk factors with emphasis on radiation parameters and chemotherapy. *Int J Radiat Oncol Biol Phys.* 2006;65:499–508.
9. Levivier M, Becerra A, De Witte O, Brotchi J, Goldman S. Radiation necrosis or recurrence. *J Neurosurg.* 1996;84:148–149.
10. Clarke JL, Chang S. Pseudoprogression and pseudoresponse: challenges in brain tumor imaging. *Curr Neurol Neurosci Rep.* 2009;9:241–246.
11. Stockham AL, Tievsky AL, Koyfman SA, et al. Conventional MRI does not reliably distinguish radiation necrosis from tumor recurrence after stereotactic radiosurgery. *J Neurooncol.* 2012;109:149–158.
12. Kang TW, Kim ST, Byun HS, et al. Morphological and functional MRI, MRS, perfusion and diffusion changes after radiosurgery of brain metastasis. *Eur J Radiol.* 2009;72:370–380.
13. Chen W. Clinical applications of PET in brain tumors. *J Nucl Med.* 2007;48: 1468–1481.
14. Chao ST, Suh JH, Raja S, Lee SY, Barnett G. The sensitivity and specificity of FDG PET in distinguishing recurrent brain tumor from radionecrosis in patients treated with stereotactic radiosurgery. *Int J Cancer.* 2001;96:191–197.
15. Ricci PE, Karis JP, Heiserman JE, Fram EK, Bice AN, Drayer BP. Differentiating recurrent tumor from radiation necrosis: time for re-evaluation of positron emission tomography? *AJNR Am J Neuroradiol.* 1998;19:407–413.
16. Tsuyuguchi N, Sunada I, Iwai Y, et al. Methionine positron emission tomography of recurrent metastatic brain tumor and radiation necrosis after stereotactic radiosurgery: is a differential diagnosis possible? *J Neurosurg.* 2003;98: 1056–1064.
17. Grosu AL, Astner ST, Riedel E, et al. An interindividual comparison of *O*-(2-[^{18}F]fluoroethyl)-L-tyrosine (FET)- and L-[methyl-^{11}C]methionine (MET)-PET in patients with brain gliomas and metastases. *Int J Radiat Oncol Biol Phys.* 2011;81:1049–1058.
18. Chen W, Silverman DH, Delaloye S, et al. ^{18}F-FDOPA PET imaging of brain tumors: comparison study with ^{18}F-FDG PET and evaluation of diagnostic accuracy. *J Nucl Med.* 2006;47:904–911.
19. Namavari M, Bishop A, Satyamurthy N, Bida G, Barrio JR. Regioselective radiofluorodestannylation with [^{18}F]F_2 and [^{18}F]CH_3COOF: a high yield synthesis of 6-[^{18}F]fluoro-L-dopa. *Int J Rad Appl Instrum A.* 1992;43:989–996.
20. Bishop A, Satyamurthy N, Bida G, Hendry G, Phelps M, Barrio JR. Proton irradiation of [^{18}O]O_2: production of [^{18}F]F_2 and [^{18}F]F_2 + [^{18}F]OF_2. *Nucl Med Biol.* 1996;23:189–199.
21. Bergström M, Litton J, Eriksson L, Bohn C, Blomqvist G. Determination of object contour from projections for attenuation correction in cranial positron emission tomography. *J Comput Assist Tomogr.* 1982;6:365–372.
22. Kinahan PE, Townsend DW, Beyer T, Sashin D. Attenuation correction for a combined 3D PET/CT scanner. *Med Phys.* 1998;25:2046–2053.
23. Nuyts J, Michel C, Dupont P. Maximum-likelihood expectation-maximization reconstruction of sonograms with arbitrary noise distribution using NEC-transformations. *IEEE Trans Med Imaging.* 2001;20:365–375.
24. Peterson AM, Meltzer CC, Evanson EJ, Flickinger JC, Kondziolka D. MR imaging response of brain metastases after gamma knife stereotactic radiosurgery. *Radiology.* 1999;211:807–814.
25. Macdonald DR, Cascino TL, Schold SC Jr, Cairncross JG. Response criteria for phase II studies of supratentorial malignant glioma. *J Clin Oncol.* 1990;8: 1277–1280.
26. Patronas NJ, Di Chiro G, Brooks RA, et al. Work in progress: [^{18}F]fluorodeoxyglucose and positron emission tomography in the evaluation of radiation necrosis of the brain. *Radiology.* 1982;144:885–889.
27. Fulham MJ, Brunetti A, Aloj L, Raman R, Dwyer AJ, Di Chiro G. Decreased cerebral glucose metabolism in patients with brain tumors: an effect of corticosteroids. *J Neurosurg.* 1995;83:657–664.
28. Spence AM, Muzi M, Mankoff DA, et al. ^{18}F-FDG PET of gliomas at delayed intervals: improved distinction between tumor and normal gray matter. *J Nucl Med.* 2004;45:1653–1659.
29. Horky LL, Hsiao EM, Weiss SE, Drappatz J, Gerbaudo VH. Dual phase FDG-PET imaging of brain metastases provides superior assessment of recurrence versus post-treatment necrosis. *J Neurooncol.* 2011;103:137–146.
30. Heiss WD, Wienhard K, Wagner R, et al. F-DOPA as an amino acid tracer to detect brain tumors. *J Nucl Med.* 1996;37:1180–1182.
31. Schiepers C, Chen W, Cloughesy T, Dahlbom M, Huang SC. ^{18}F-FDOPA kinetics in brain tumors. *J Nucl Med.* 2007;48:1651–1661.
32. Oldendorf WH, Szabo J. Amino acid assignment to one of the three blood-brain barrier amino acid carriers. *Am J Physiol.* 1976;230:94–98.
33. Wade LA, Katzman R. Synthetic amino acids and the nature of L-DOPA transport at the blood-brain barrier. *J Neurochem.* 1975;25:837–842.
34. Kumakura Y, Cumming P. PET studies of cerebral levodopa metabolism: a review of clinical findings and modeling approaches. *Neuroscientist.* 2009;15:635–650.
35. Terakawa Y, Tsuyuguchi N, Iwai Y, et al. Diagnostic accuracy of ^{11}C-methionine PET for differentiation of recurrent brain tumors from radiation necrosis after radiotherapy. *J Nucl Med.* 2008;49:694–699.
36. Galldiks N, Stoffels G, Filss CP, et al. Role of *O*-(2-^{18}F-fluoroethyl)-L-tyrosine PET for differentiation of local recurrent brain metastasis from radiation necrosis. *J Nucl Med.* 2012;53:1367–1374.
37. Patil CG, Pricola K, Sarmiento JM, Garg SK, Bryant A, Black KL. Whole brain radiation therapy (WBRT) alone versus WBRT and radiosurgery for the treatment of brain metastases. *Cochrane Database Syst Rev.* 2012;(9):CD006121.
38. Roelcke U, Radu EW, von Ammon K, Hausmann O, Maguire RP, Leenders KL. Alteration of blood-brain barrier in human brain tumors: comparison of [^{18}F] fluorodeoxyglucose, [^{11}C]methionine and rubidium-82 using PET. *J Neurol Sci.* 1995;132:20–27.